

FEALPy v3: A Cross-platform Intelligent Numerical Simulation Engine

Yangyang Zheng¹, Huayi Wei^{1,3,*}, Yunqing Huang^{1,2}, Chunyu Chen⁴, Tian Tian⁵, Hanbin Liu¹, Wenbin Wang¹ and Liang He¹

¹ School of Mathematics and Computational Sciences, Xiangtan University, Hunan 411105, P.R. China ² National Center for Applied Mathematics in Hunan, Xiangtan 411105, P. R. China ³ Hunan Key Laboratory for Computation and Simulation in Science and Engineering Xiangtan 411105, China ⁴ School of Mathematical Sciences, Peking University, Beijing 100871, China ⁵ Shenzhen International Center For Industrial And Applied Mathematics; Shenzhen Research Institute of Big Data; School of Science and Engineering, Chinese University of Hong Kong (Shenzhen); Guang Dong 518172, China

Abstract. In recent years, the software ecosystem for numerical simulation still remains fragmented, with different algorithms and discretization methods often implemented in isolation, each with distinct data structures and programming conventions. This fragmentation is compounded by the growing divide between packages from different research fields and the lack of a unified, universal data structure, hindering the development of integrated, cross-platform solutions. In this work, we introduce FEALPy, a numerical simulation engine built around a unified tensor abstraction layer in a modular design. It enables seamless integration between diverse numerical methods along with deep learning workflows. By supporting multiple computational backends such as NumPy, PyTorch, and JAX, FEALPy ensures consistent adaptability across CPU and GPU hardware systems. Its modular architecture facilitates the entire simulation pipeline, from mesh handling and assembly to solver execution, with built-in support for automatic differentiation. In this paper, the versatility and efficacy of the framework are demonstrated through applications spanning linear elasticity, high-order PDEs, moving mesh methods, inverse problems and path planning.

AMS subject classifications: 65N30, 65N50, 65Y15, 65Z05, 65M60

Key words: numerical simulation, software engineering, multiple backends, multiple fields, modular design.

*Corresponding author. *Email addresses:* 202531510218@smail.xtu.edu.cn (Y. Zheng), weihuayi@xtu.edu.cn (H. Wei) huangyq@xtu.edu.cn (Y. Huang), cbtxs@math.pku.edu.cn (C. Chen), tiantian00@cuhk.edu.cn (T. Tian), 202431510132@smail.xtu.edu.cn (H. Liu), 202531510193@smail.xtu.edu.cn (W. Wang), lianghe@smail.xtu.edu.cn (L. He),

1 Introduction

Numerical computing software plays a central role in solving a wide range of scientific and engineering problems. Many such problems are governed by partial differential equations (PDEs), whose solution spaces are inherently infinite-dimensional. To make these problems computable on digital hardware with finite memory, numerical discretization methods—such as the finite element method (FEM), finite difference method (FDM), and finite volume method (FVM)—approximate infinite-dimensional spaces with finite ones. The success of these methods has enabled accurate simulations of physical systems in diverse fields, from fluid dynamics to solid mechanics.

However, the software ecosystem for numerical simulation remains fragmented. Different algorithms are often implemented independently, each with its own data structures, programming standards, and interface conventions. At the same time, the growing diversity of computing hardware—from CPUs and GPUs to specialized accelerators—introduces additional complexity. Algorithms must be adapted to distinct programming models and memory hierarchies, making cross-platform compatibility and performance portability major challenges. As a result, reproducing and extending numerical methods across heterogeneous environments is cumbersome and error-prone.

In recent years, deep learning (DL) has brought new paradigms to scientific computing. Neural networks (NNs) can approximate complex mappings from data, offering a data-driven complement to traditional physics-based approaches. Yet, traditional numerical software and DL frameworks remain largely disconnected—most numerical solvers rely on mesh-based data structures, while DL systems such as PyTorch and TensorFlow operate primarily on tensors. This incompatibility hinders seamless integration between the two paradigms.

Interestingly, many core operations in numerical methods can naturally be expressed as tensor computations. Quantities such as fields, basis functions, and element matrices can all be represented as multi-dimensional arrays attached to mesh entities. Fundamental operations—indexing, reduction, concatenation, and Einstein summation—are shared between numerical algorithms and neural network training. This theoretical overlap opens a path toward unifying traditional numerical computation and modern tensor-based DL frameworks.

Mature numerical PDE software such as iFEM [11], AFEPack [8], MFEM [3], FEniCSx [2,5,32,33], deal.II [4], PHG, and OpenFOAM [21] offer powerful and well-established infrastructures for numerical simulation. These software systems have greatly advanced the development and deployment of high-performance PDE solvers across many scientific and engineering domains. While emerging demands—such as unified tensor representations, interaction with modern DL toolchains, and cross-backend portability—call for complementary approaches that extend beyond the traditional designs of existing packages.

Motivated by this observation, we have developed FEALPy, a tensor-centric numerical simulation engine designed for flexibility, interoperability, and extensibility.

FEALPy builds a unified abstraction layer over multiple tensor computation backends (including NumPy [16], PyTorch [29], JAX [6] and more in the future), enabling consistent data flow across heterogeneous hardware architectures. Its modular design decouples low-level tensor operations from higher-level algorithmic modules—such as meshes, function spaces, discretization schemes, and solvers—allowing users to implement complex simulation workflows with concise and reusable code. By adopting a unified tensor interface, FEALPy provides a common computational foundation for both classical numerical algorithms and differentiable programming. It supports automatic differentiation (AD) throughout the entire pipeline, making it possible to embed finite element solvers as differentiable layers within NNs. This integration bridges the gap between traditional physics-based modeling and data-driven learning, advancing the convergence of numerical simulation and modern AI.

The remainder of this paper is organized as follows. Section 2 introduces the overall software architecture and data structure of FEALPy. Section 3 discusses implementation details and programming techniques. Section 4 demonstrates applications of FEALPy in diverse fields, including elasticity, high-order PDEs, moving mesh, operator learning, and optimization. Section 5 presents two application frameworks, SOPTX and FractureX, developed on top of FEALPy. Section 6 concludes the paper by summarizing the main contributions and discussing the future directions.

2 Software Architecture and Data Structure

2.1 Overview

FEALPy is a modular numerical simulation engine built around tensorized computing. Its architecture separates mathematical abstractions from computational details so that numerical algorithms remain independent of specific hardware or software backends. Based on the dependencies between tensors, geometry, algorithms and applications, from bottom to top, we divide FEALPy into four layers: tensor layer, commonality layer, algorithm layer and field layer, see Fig. 1. The tensor layer provides an abstract interface to meet the needs of all upper modules that are based on tensor computations; the commonality layer provides basic data structures and algorithms, such as meshes, function spaces, sampling, integration and solvers; the algorithm layer provides many classic numerical algorithm frameworks, such as FEM, FDM, FVM, SPH; the field layer enters each specific field and provides common material settings, physical models, computational models and examples.

2.2 Backend Module and Hardware Adaptation

The backend layer is the foundation of FEALPy’s interoperability. It provides a backend manager (BM) that standardizes tensor operation interfaces across multiple frameworks. Every tensor operation in FEALPy—such as array creation, broadcasting, reduction, or Einstein summation—is routed through this manager, which dynamically

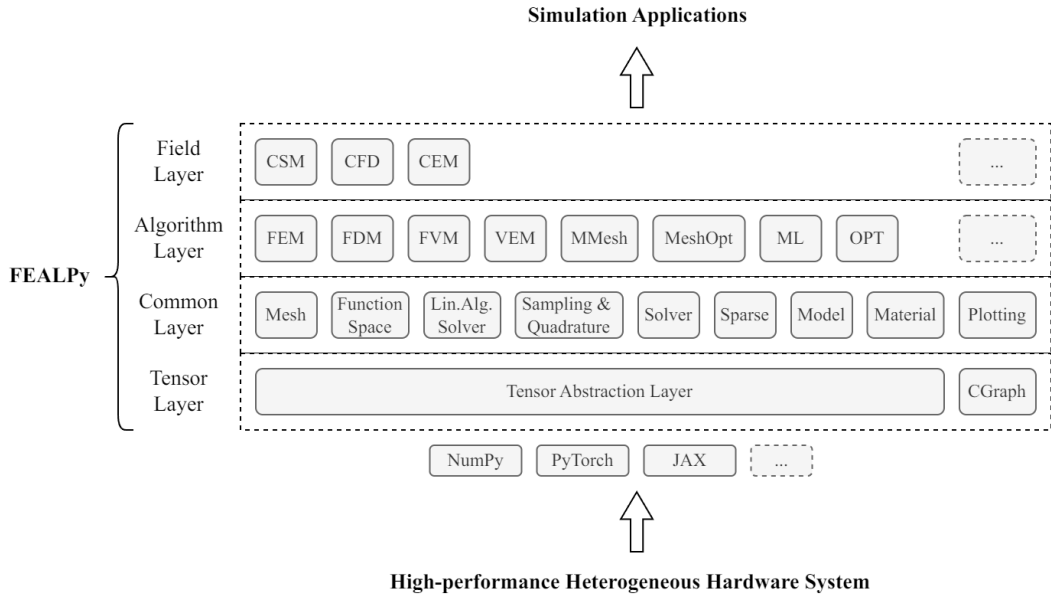


Figure 1: Software architecture of FEALPy

dispatches calls to the active backend. This design mirrors the multi-backend philosophy adopted by TensorLy [23], where the same high-level logic can execute on CPUs or GPUs without code modification.

Backend layer exposes a unified API compatible with the Python Array API Standard [1]. It abstracts the complexities of managing different tensor computation backends, allowing FEALPy to integrate various libraries such as NumPy, PyTorch, JAX, MindSpore, PaddlePaddle, and others. This flexibility ensures that users can seamlessly adapt their simulations to the most suitable tensor backend based on specific hardware requirements. In addition, as all higher-level modules operate solely on BM to access APIs, FEALPy ensures that algorithms written once in terms of abstract tensor operations can be executed on any supported backend. This not only simplifies development by providing a unified API, but also ensures long-term maintainability and adaptability as new backends and hardware architectures emerge.

Key features include:

- **Unified Data Structure:** All computations—from finite element assembly to NN operations—are performed on unified tensors, eliminating format conversions and device transfers.
- **Batch Processing:** The framework supports mini-batch processing of multiple PDE solutions simultaneously, leveraging parallelized computation on GPU architectures.
- **Automatic Differentiation (AD):** FEALPy enables gradient computation through the entire pipeline, allowing the FEM solver to function as a differentiable layer

within NNs.

This backend abstraction isolates algorithmic logic from low-level performance tuning, allowing the same solver implementation to benefit from backend-specific optimizations such as GPU kernels or just-in-time compilation. It thus forms the computational backbone of FEALPy’s multi-paradigm design: a consistent numerical environment adaptable to both classical PDE solvers and AI-driven applications.

2.3 Common Modules with Unified Interfaces

Common modules such as meshes, function spaces, linear algebra solvers, samplers, and integrators are implemented based on the tensor abstraction layer. They defines the essential abstractions shared by different discretization methods, ensuring that higher-level algorithms operate consistently across problem types and backends. The most significant features of these modules are their almost unified interfaces and strong extensibility, which are particularly emphasized in the design of FEALPy so that users can have a consistent experience when developing extensions and higher-level modules.

At its center is the Mesh module, which handle the geometric and topological structure of computational domains. The `Mesh` type is an abstract canonical interface that provides prescribed geometric and topological information for other modules. Mesh objects describe nodes, edges, faces, and cells, and store mappings between these entities. FEALPy supports both structured and unstructured meshes in 1, 2, and 3 dimensions, along with flexible boundary tagging for applying boundary conditions. All mesh data are stored based on tensors, enabling efficient vectorized operations and direct interaction with the backend layer.

The Function Space module manages function space types, usually based on meshes, to discrete the solution of problems. The `Function Space` type is an abstract interface that defines a set of functions as the basis, including their values, gradients, and Hessian matrices, and provides a global index of these functions. This abstraction allows algorithms such as FEM assembly or gradient evaluation to be expressed purely through tensor operations, independent of the specific discretization method. Different function space subclasses correspond to different function definitions and global indexing methods, which can serve various types of finite elements, finite volumes, and even random neural networks, with the same interface, supporting numerical integration and sampling on functions.

In addition to mesh and function-space management, the common layer includes a set of modules that serve as reusable building blocks across the framework:

- `Solver`: A variety of algebra solvers for linear systems.
- `Sparse`: A variety of sparse formats, including CSR, CSC, and COO, supports multiple backends.
- `Quadrature`: Generate quadrature rules for numerical integration.

- **Plotting:** Supplies lightweight visualization tools for quick inspection of meshes and values attached to their entities.

Together, these components form a coherent foundation on which discretization methods can be built. Their tensor-based design ensures consistency and extensibility: new numerical schemes can be implemented by reusing these common abstractions rather than redefining data structures or computation patterns.

2.4 Basic Algorithms Implemented through Tensor Calculation

The basic algorithm layer contains a variety of common numerical method modules. Every computation in this layer, from local element assembly to global matrix construction, is formulated as tensor operations that can be executed on any supported backend. FEM is one of the oldest modules and the starting point for the development of FEALPy.

The data flow in FEM consists mainly of numerical integration to form element matrices, global assembly of linear systems, and enforcement of boundary conditions. In FEALPy, these processes are organized around three core components: Integrators, Forms, and Boundary Condition Processors.

- **Integrators:** evaluate local quantities, typically integrals of basis functions and their derivatives over mesh entities, and return results as element-level tensors. Specialized implementations can also compute fluxes across control-volume interfaces, enabling reuse within FVM formulations.
- **Forms:** combine element matrices with global indexing information provided by the Function Space module, managing the insertion of nonzero entries into sparse matrices.
- **Boundary Condition Processors:** modify assembled systems according to Dirichlet constraints.

Because all these components operate on tensors, algorithms remain independent of backends and can automatically benefit from hardware acceleration or automatic differentiation. This abstraction also facilitates the extension of existing methods: developers can prototype new variational forms or discretization strategies simply by redefining integrators or function spaces without altering the rest of the framework.

2.5 The Field Layer: Packaging for Fields

Built on top of the tensor, common, and algorithmic layers, the field layer serves as the application interface of FEALPy, where developers and users can develop specialized subclasses for specific domains. It organizes domain-specific modules for various areas of computational science and engineering, such as solid mechanics, fluid dynamics, and electromagnetics. Each module provides commonly used material models,

constitutive relations, boundary conditions, and example problems tailored to its discipline.

While the present paper focuses on the general software architecture and tensor-based design of FEALPy, further details of these field-specific extensions will be discussed in companion works.

3 Implementation Details and Programming Techniques

3.1 Backend Manager and Adaptors

A significant advantage of FEALPy’s Tensor Backend System is its seamless backend switching capability. Users can optimize simulations for different computing environments—whether they are running simulations on CPUs, GPUs, or specialized hardware like TPUs—without modifying their codebase. The Lst. 1 snippet demonstrates how FEALPy enables users to switch between different tensor backends with minimal effort. This seamless switching capability allows developers to experiment with various backends and select the one that offers the best performance for their hardware, ensuring optimized simulation results.

```

1 from fealpy.backend import bm
2 from fealpy.mesh import UniformMesh
3 bm.set_backend("pytorch")
4 mesh = UniformMesh([0, 1, 0, 1], nx=10, ny=10)
5 print(type(mesh.entity('cell')))
```

Listing 1: Switching between different tensor backends: By replacing the backend name passed to the `set_backend` function, the object type of the output tensor changes. `bm` here refers to the backend manager, which provides standard array APIs.

How does the Backend module build a tensor abstraction layer so that users can operate multiple tensor libraries through almost the same interface? Constructed by a backend manager and several backend adaptors, the Backend module has two working steps: transmission and translation.

`BackendManager` is a router that calls tensor operations of the selected version, and the corresponding adaptor is initialized if it has not been loaded yet. This lazy loading feature avoids unnecessary importation.

While `Adaptors` are translators that simulate the standard interface based on the corresponding tensor library. Three cases are considered in each interface implementation: (1) satisfied by a function in the tensor library: then the function is directly referenced in the adapter; (2) satisfied at the functional level, but with a different function name: then the function is referenced in the adapter via a mapping table; (3) not satisfied: then manual implementation based on the corresponding tensor library is required in the adapter.

This super-polymorphic feature between different tensor libraries will give the same ability to switch between tensor libraries for almost all implementations of high-level modules, such as those presented in the following subsections.

3.2 Mesh Data Structure Based on Tensors

Based on the tensor abstraction interface, we designed the mesh data structure in FEALPy carefully. The Cartesian coordinate of points are recorded in a floating-point tensor, which is then combined into higher-dimensional shapes through a series of non-negative integer tensors. We adopt the notation shown in Tab. 1.

Notation	Description
GD	Geometry dimensions
TD	Topological dimensions
NN	Number of nodes
NE	Number of edges
NF	Number of faces
NC	Number of cells

Table 1: Common notations in FEALPy. Node, edge, face and cell are mesh entities.

Nodes. The position of a node is determined by a vector of length GD, so all nodes in a mesh is stored as a tensor with shape [NN, GD]. Once the tensor is stored, not only the node positions are identified, but also their global indices.

Line segments, triangles and quadrangles. Two vertices can form a line segment by connecting them in a directed way, so a 2-tuple containing the global indices of the start and end points can represent an edge. Edges of a mesh can be represented as a tensor with shape [NE, 2] in almost all unstructured mesh types in FEALPy. 2D triangles are constructed in FEALPy by connecting three vertices in counter-clockwise order, thus [num_triangles, 3] records a collection of them in a mesh. See Lst.2 as an example for a mesh containing 2 triangles divided from a square, and the rules for other shapes are similar.

```

1 from fealpy.mesh import TriangleMesh
2 node = bm.tensor([
3     [0. 0.] # 0
4     [0. 1.] # 1
5     [1. 0.] # 2
6     [1. 1.] # 3
7 ], dtype=bm.float64)
8 cell = bm.tensor([
9     [2 3 0] # 0
10    [1 0 3] # 1
11 ], dtype=bm.int64)
12 mesh = TriangleMesh(node, cell)

```

Listing 2: A triangular mesh is stored as two tensors—node and cell

Polygons. Polygons describe a group of shapes with inconsistent numbers of edges, and these shapes cannot be combined to form 2D tensors similar to the rules for triangles and quadrangles. All vertices from multiple polygons are directly arranged in a 1D tensor, and a pointer tensor is used to record the starting position (with an additional total number of vertices as the last element) of each polygon, as shown in Fig. 2. The length of this pointer tensor is exactly $\text{num_polygons} + 1$, like the `indptr` in CSR format sparse matrices.

Orientation. In the case of unstructured meshes, FEALPy always forms these topological 2-dimensional shapes by ordering the vertices in a circular manner, so it is natural to define the orientation by the ordering direction. The right-hand rule is used to define the orientation in FEALPy. See Fig. 3.

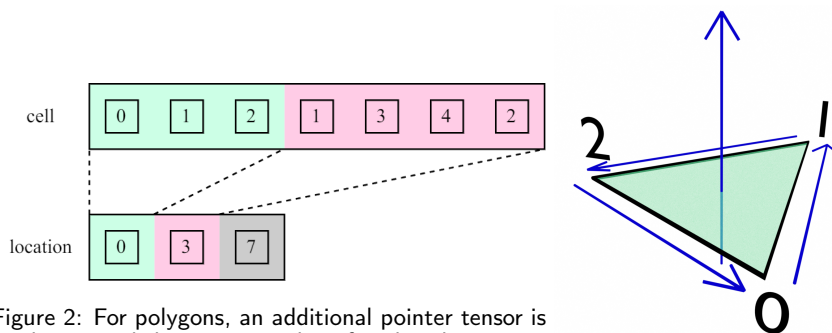


Figure 2: For polygons, an additional pointer tensor is used to record the starting index of each polygon.

Figure 3: Orientation of a 3D triangle is defined by the right-hand rule.

Mesh entities. FEALPy is more inclined to regard these organizations of nodes as entities by their topological dimensions, instead of their shapes. Nodes—which only have positional information—are 0-dimensional entities, while edges are 1-dimensional entities. Cells refer to entities with the highest topological dimension, such as any triangle in a triangular mesh. Faces refer to entities which is 1 less dimensional than cells, and they usually locate on mesh boundaries or interfaces between cells. The topological dimension of cells (i.e. the highest topological dimension) is also the topological dimension of the mesh. In particular, edges and faces refer to the same kind of entities in a topologically 2D mesh.

Topological relations. A deduplication process is needed in the mesh construction, because edges and faces are bound to have duplicates if they are simply collected from all cells. In particular, a face is definitely adjacent to two cells wanted by FEALPy to construct a topological relationship named `face_to_cell` in the shape of $[\text{NF}, 4]$. Tab. 2 shows what this four columns mean. FEALPy deduplicates the lower-dimensional entities using `lexsort`, through which the first and the last occurrences of the same

faces are extracted from the total. Since the right-hand rule is used for 2D face orientation, the cell where a face firstly appears is the cell the face faces to; and since the counter-clockwise rule is used for 1D edge orientation, the cell where an edge firstly appears is the cell on the left side of the edge.

0	1	2	3
cells indices	cells indices	local indices	local indices
left/front	right/back	left/front	right/back

Table 2: Definition of the 4 columns in `face_to_cell`. Once the indices in total faces are extracted, cell indices and local indices can be deduced by floor division and modulo.

Mesh classes. By grouping various entities together and adding related methods, a mesh class can be constructed. All supported mesh types are listed in Tab.3. The Mesh module is designed to maximize the reuse of methods through an reasonable inheritance structure and keep the interface of methods consistent between different mesh types. Therefore, meshes can be simply replaced without the need to adapt the rest of the script. See Lst.3.

Cell Type	TD	Cell Type	TD	Mesh Type	TD
Half Edge	1	Edge	1	Dart Mesh	2/3
Interval	1	Triangle	2	Uniform Mesh	1/2/3
Quadrangle	2	Polygon	2		
Tetrahedron	3	Hexahedron	3		
Prism	3	Node	0		
Lagrange Triangle	2	Lagrange Quadrangle	2		
Lagrange Tetrahedron	3	Lagrange Hexahedron	3		

Table 3: Mesh types of unstructured (left and middle columns) and others (right column) in FEALPy and their supported TDs.

```

1 from fealpy.mesh import TriangleMesh, QuadrangleMesh
2 from fealpy.functionspace import LagrangeFESpace
3
4 if meshtype == "TRIA":
5     mesh = TriangleMesh.from_box()
6 elif meshtype == "QUAD":
7     mesh = QuadrangleMesh.from_box()
8 else:
9     raise ValueError()
10
11 space = LagrangeFESpace(mesh, p=1)
12 ...

```

Listing 3: The mesh type can be simply replaced directly. The code shows the replacement from `TriangleMesh` to `QuadrangleMesh`.

3.3 Basis and DoF Management

Numbering the global degrees-of-freedom (DoF) and inferring their relationships with local DoFs in mesh entities is called DoF management in FEALPy.

For most finite element methods or their variants, DoFs are arranged by interpolation points on the mesh entities, and there are two main types of DoF management provided in FEALPy in this way. The first type is continuous, where adjacent mesh cells may share a part of DoFs at their interface. Section 6 of [10] has discussed the global indexing rules for Lagrange interpolation points in detail, which is actually the main idea behind FEALPy's implementation of various finite element DoF management. In order to provide a non-repeating numbering that is as consistent as possible for all mesh entities, we adopt the order of DoFs from low-dimensional entities to high-dimensional entities in the order of "node-edge-face-cell", as shown in Fig. 4. When numbering the DoFs inside two adjacent cells, the DoFs at their interface are already numbered. The second type is discontinuous, where adjacent mesh cells do not share any DoF. Non-repeating numbers can be generated directly from the correspondence between cells and their local DoFs.

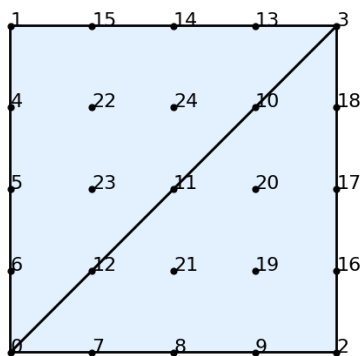


Figure 4: Example of global DoF numbering ($p=4$) in a triangle in FEALPy.

Take the Lagrange space as an example—both basis generation and DoF management in 1, 2, and 3 dimensions can be supported in FEALPy with arbitrary order. Because they are both constructed from the multiple indices on mesh entities, which are generated as a multi-dimensional tensor, independent of the spatial dimensions and the order of the indices.

Based on different basis function implementations and mappings of local-global DoFs, FEALPy already supports a variety of function spaces summarized in Tab. 4.

3.4 Sampling and Quadrature

Sampling and quadrature are also essential tools for many numerical methods. The Quadrature module stores precomputed barycentric coordinates of quadrature points

Element Types	GD	References
Lagrange	Any	
Bernstein	Any	[22]
C^m Conforming	2, 3	[9, 12, 18]
Hu-Zhang	2, 3	[19]
First Nédélec	2, 3	[28]
Second Nédélec	2, 3	[28], [10]
Raviart-Thomas	2, 3	[30]
Brezzi-Douglas-Marini	2, 3	[7], [10]
Parametric Lagrange	Any	

Table 4: Element types in FEALPy and their supported GDs.

and their weights generated from symmetric quadrature rules on simplexes [35], including line segments, triangles, and tetrahedrons. While quadrature points on d -hypercubes, such as quadrangles and hexahedrons, are generated via tensor products of 1D Gauss-Legendre quadrature rules. Similarly, triangular prisms and pyramids can also get their quadrature rules via tensor products. Lst.4 gives an example.

```

1 quad_pts = (quad_pts_1d_a, quad_pts_1d_b)
2 weights = bm.einsum(
3     'i,j->ij', weights_1d_a, weights_1d_b
4 ).reshape(-1)

```

Listing 4: Quadrature points on quadrangles can be generated via tensor products of two 1D Gauss-Legendre quadrature rules.

Samplers are designed for generating equidistant or random collocation points for function learning and operator learning. Sampling can be done mesh-independent, which is different from the Quadrature module, as a path of circumventing the curse of dimensionality.

3.5 Sparse Format and Matrix Assembly

Sparse COO and CSR formats are implemented in FEALPy and can work on any tensor library supported by FEALPy, as they are completely based on the tensor data structure and is decoupled with any specific backends.

Extended sparse matrix formats. Let d be the dimension (number of axes) and mnz be the number of non-zeros. In both COO and CSR, FEALPy allows `None` data (matrices with bool elements, for sparse adjacency) and data with a batch axis as the 0-axis, as shown in Fig. 5.

Batched matrix assembly. Combining the cell matrix from Integrator and the DoF management from the `FunctionSpace`, `Forms` in the FEM module manages to arrange the non-zero elements in sparse linear systems leveraging the Sparse module. Lst.5 gives an example to explain the arrangement.

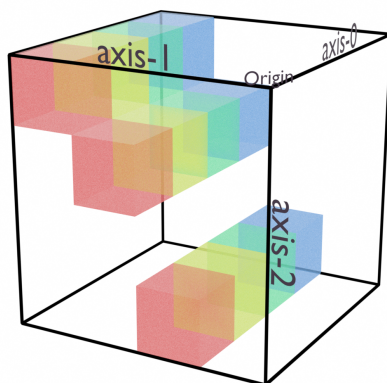


Figure 5: Hybrid COO: a batched sparse matrix containing many sparse matrices with the same non-zero pattern. This is useful in assembling matrices for batches of equations with different coefficients in FEM.

```

1 I = bm.broadcast_to(ve2dof[:, :, None], local_shape)
2 J = bm.broadcast_to(ue2dof[:, None, :], local_shape)
3 indices = bm.stack([I.ravel(), J.ravel()], axis=0)
4 cell_matrix = bm.reshape(cell_matrix, (-1,))
5 # The shape will be (batch_size, -1) for batched assembly.
6 M = M.add(COOTensor(indices, cell_matrix, sparse_shape))

```

Listing 5: Assembly of global stiffness matrices. The `local_shape` equals to `(num_cells, num_quadpts, num_basis, num_basis)` which stores the shape of `cell_matrix`; `ue2dof` and `ve2dof` are DoF maps, in the shape of `(num_cells, num_dofs)`.

Unfortunately, to our best knowledge, matrix-vector multiplication of batched sparse matrices is not well supported now by any tensor computation library at the C/C++ level. Although implementations based on standard tensor computation at the Python level can output correct results, a significant loss of efficiency can be observed in solvers.

4 Numerical Examples

4.1 3D Linear Elasticity Problem with Lagrange Finite Elements

This subsection presents a fundamental numerical example in solid mechanics, designed to verify the basic correctness and computational accuracy of FEALPy. Given computational domain $\Omega = [0,1]^3$, the material is modeled as a homogeneous, isotropic, linear elastic solid with Lamé constants $\lambda = 1$ and shear modulus $\mu = 1$. The governing system of equations is given by the equilibrium equation, kinematic strain-

displacement relation, and the constitutive law (Generalized Hooke's Law):

$$-\nabla \cdot \boldsymbol{\sigma} = \mathbf{b} \quad \text{in } \Omega \quad (4.1)$$

$$\boldsymbol{\varepsilon} = \frac{1}{2}(\nabla \mathbf{u} + (\nabla \mathbf{u})^T) \quad (4.2)$$

$$\boldsymbol{\sigma} = \lambda \text{tr}(\boldsymbol{\varepsilon}) \mathbf{I} + 2\mu \boldsymbol{\varepsilon} \quad (4.3)$$

where \mathbf{u} is the displacement vector, $\boldsymbol{\varepsilon}$ is the strain tensor, and $\boldsymbol{\sigma}$ is the Cauchy stress tensor. The exact displacement field $\mathbf{u} = (u_1, u_2, u_3)$ is chosen to be:

$$\mathbf{u} = \begin{bmatrix} 200\mu(x-x^2)^2(2y^3-3y^2+y)(2z^3-3z^2+z) \\ -100\mu(y-y^2)^2(2x^3-3x^2+x)(2z^3-3z^2+z) \\ -100\mu(z-z^2)^2(2y^3-3y^2+y)(2z^3-3z^2+z) \end{bmatrix}$$

The corresponding body force density \mathbf{b} , which satisfies the equilibrium equation above, is derived accordingly and is:

$$\mathbf{b} = \begin{bmatrix} -400\mu(2y-1)(2z-1)[3(x^2-x)^2(y^2-y+z^2-z) + (1-6x+6x^2)(y^2-y)(z^2-z)] \\ 200\mu(2x-1)(2z-1)[3(y^2-y)^2(x^2-x+z^2-z) + (1-6y+6y^2)(x^2-x)(z^2-z)] \\ 200\mu(2x-1)(2y-1)[3(z^2-z)^2(x^2-x+y^2-y) + (1-6z+6z^2)(x^2-x)(y^2-y)] \end{bmatrix}$$

A non-homogeneous Dirichlet boundary condition is applied over the entire boundary $\partial\Omega$.

In discretization, the domain Ω was initially partitioned into a uniform $4 \times 4 \times 4$ mesh of tetrahedrons, and was successively uniformly refined four times. Finite element spaces $V_h \subset H^1(\Omega)$ was constructed using linear or quadratic Lagrange elements on each mesh level. Lst. 6 shows the construction of the finite element space.

```

1 from fealpy.mesh import TetrahedronMesh
2 from fealpy.functionspace import (
3     LagrangeFESpace, TensorFunctionSpace
4 )
5 mesh = TetrahedronMesh.from_box(box=domain, nx=4, ny=4, nz=4)
6 space = LagrangeFESpace(mesh=mesh, p=1, ctype='C')
7 tensor_space = TensorFunctionSpace(space, shape=(-1, 2))

```

Listing 6: A tensor function space with DoFs shaped (2,) was constructed on a tetrahedral mesh.

The weak formulation of the problem is: Find $\mathbf{u}_h \in V_h$ such that

$$\int_{\Omega} \boldsymbol{\sigma}(\mathbf{u}_h) : \boldsymbol{\varepsilon}(\mathbf{v}_h) d\Omega = \int_{\Omega} \mathbf{b} \cdot \mathbf{v}_h d\Omega \quad \forall \mathbf{v}_h \in V_h^0$$

where V_h^0 is the test space satisfying homogeneous Dirichlet boundary conditions. See Lst. 7 for the code. The non-homogeneous Dirichlet conditions are enforced in a strong form.

```

1 from fealpy.fem import BilinearForm, LinearElasticIntegrator
2 from fealpy.material import IsotropicLinearElasticMaterial
3

```

```

4 material = IsotropicLinearElasticMaterial(
5     lame_lambda=1.0,
6     shear_modulus=1.0,
7     plane_type='plane_strain',
8 )
9 bform = BilinearForm(tensor_space)
10 bform.add_integrator(
11     LinearElasticIntegrator(material=material)
12 )
13 A = bform.assembly()

```

Listing 7: Construct a bilinear form based on the space, and integrators can be added to the form to define the weak form. The assembly method returns a sparse matrix. The construction of linear forms is similar.

The accuracy of FEALPy's computation was quantified by calculating the L^2 -norm error of the displacement:

$$\text{Error} = \|\mathbf{u}_{\text{exact}} - \mathbf{u}_h\|_{L^2(\Omega)}$$

The computed L^2 errors and the corresponding mesh sizes are summarized in Tab. 5.

		h	1/4	1/8	1/16	1/32	1/64
$p=1$	DoF		375	2187	14739	107811	823875
	$\ \mathbf{u}_{\text{exact}} - \mathbf{u}_h\ _{L^2(\Omega)}$		3.0271e-2	1.1616e-2	3.5874e-3	9.8912e-4	2.5827e-4
	Order		-	1.3818	1.6951	1.8587	1.9372
$p=2$	DoF		2187	14739	107811	823875	-
	$\ \mathbf{u}_{\text{exact}} - \mathbf{u}_h\ _{L^2(\Omega)}$		5.0775e-3	6.0218e-4	6.8054e-5	7.9984e-6	-
	Order		-	3.0759	3.1454	3.0889	-

Table 5: Convergence results for the linear elasticity problem. The error decreases systematically as the mesh is refined.

The calculated convergence rate approaches the optimal theoretical rate 2 for linear elements, and 3 for quadratic elements in the L^2 -norm, which strongly validates the correct implementation of the FEM for linear elasticity within FEALPy and confirms its numerical precision.

4.2 3D Biharmonic Equation with Smooth Finite Elements

The biharmonic equation arises in models of thin plate deformation and Stokes flow problems. Here, the following problem is considered on a unit cube domain $\Omega = (0,1)^3$:

$$\Delta^2 u = f$$

with manufactured solution $u_{\text{exact}} = \sin(4x)\sin(4y)\sin(4z)$, and Dirichlet boundary conditions prescribing both u and $\partial_n u$ on $\partial\Omega$. The weak formulation requires H^2 -conforming (i.e., C^1 -continuous) finite element spaces, which are non-trivial to construct on simplicial meshes in 3D.

We use the C^1 -conforming finite element space proposed by [12, 18], with shape functions of degree $k \geq 9$ on tetrahedral meshes.

One of FEALPy’s key features is its modular design, which allows users to implement new finite elements by defining only the local basis functions and degrees of freedom, while reusing existing infrastructure for mesh handling, assembly, and linear algebra. To solve this problem, we simply replaced the standard Lagrange element with the smooth element (C^m Conforming space, implemented by [9]), on a initially $1 \times 1 \times 1$ uniform mesh of tetrahedrons. See Lst. 8.

```

1 ...
2 mesh = TriangleMesh.from_box([0, 1, 0, 1], n, n)
3 space = CmConformingFESpace2d(mesh, p, 1, isCornerNode)
4 bform = BilinearForm(space)
5 MLI = MthLaplaceIntegrator(m=2, coef=1, q=p+4)
6 bform.add_integrator(MLI)
7 A = bform.assembly()
8 ...

```

Listing 8: The Smooth Finite Element can be implemented by introducing a new function space and integrator.

Tab. 6 shows the convergence on a sequence of uniformly refined tetrahedral meshes, which confirm optimal convergence rates in the L^2 -norm, as theoretically expected.

h	1	1/2	1/4	1/8
DoF	582	2761	16791	116971
$\ u_{\text{exact}} - u_h\ _{L^2}$	6.6494e-2	6.0048e-5	7.1664e-8	5.4160e-11
Order	-	10.1129	9.7106	10.3698
$\ \nabla u_{\text{exact}} - \nabla u_h\ _{L^2(\Omega)}$	4.1421e-1	1.1596e-3	2.8335e-6	4.5102e-9
Order	-	8.4806	8.6768	9.2952
$\ \nabla^2 u_{\text{exact}} - \nabla^2 u_h\ _{L^2(\Omega)}$	3.4483e+0	2.1847e-2	1.0433e-4	3.4023e-7
Order	-	7.3023	7.7101	8.2605

Table 6: Convergence results for the 3D biharmonic equation with C^1 -tet elements, and shape functions of degree $k=9$.

This example demonstrates the flexibility of FEALPy in implementing non-standard finite elements. By leveraging a modular architecture, new elements (such as the C^1 -conforming tetrahedral element) can be integrated seamlessly — users need only provide the local basis and degree-of-freedom definitions, while all other components (e.g., assembly, boundary conditions, solvers) remain reusable.

4.3 Burgers’ Equation with Moving Mesh

The moving mesh method, also known as the r-adaptive method, relocates a fixed number of mesh nodes according to user-defined monitor functions. It has been widely applied in fields such as fluid dynamics, heat transfer, and combustion simulation, where solutions often exhibit sharp gradients or localized features, such as shock waves or boundary layers, amid relatively smooth regions. While fixed uniform meshes may fail to capture such features efficiently without excessive refinement, the moving mesh

method adaptively concentrates mesh nodes in regions of high variation, significantly improving computational accuracy and efficiency without altering the mesh topology.

In FEALPy, we have implemented a high-dimensional, vectorized moving mesh algorithm based on the Harmonic map [25,26] and the MMPDE gradient flow approach [20]. A MMesh class is provided to control the moving mesh process, as presented in Lst. 9.

```

1 from fealpy.mmesh.mmesher import MMesher
2 ...
3 mm = MMesher(mesh=mesh, uh=uh, space=space, beta=beta,
4             is_multi_phy=False, config=config)
5 mm.initialize()
6 mm.set_interpolation_method('linear')
7 mm.set_monitor('arc_length')
8 mm.set_mol_method('projector')
9 if t == 0.0: # preprocess
10     mm.set_interpolation_method('solution')
11     mm.run()
12     mm.set_interpolation_method('linear')
13 mesh, uh = mm.run()
14 uh[:] = ... # finish assembly and solve
15 mm.instance.uh = uh # update the instance

```

Listing 9: MMesh is designed to control the moving mesh process. It is irrelevant to mesh types and FE spaces.

The implementation supports both NumPy and PyTorch backends and can run on CPUs and GPUs. It is dimension-independent and allows seamless switching between mesh types, including high-order curved meshes on planes.

Let's consider a scalar Burgers' equation on $\Omega = [0,1]^2$ with time $T = [0,2]$

$$\begin{cases} \frac{\partial u}{\partial t} + u(u_x + u_y) = a\Delta u, & \mathbf{x} \in \Omega, t \in T, \\ u(\mathbf{x}, 0) = u_0(\mathbf{x}), & \mathbf{x} \in \Omega, \\ u(\mathbf{x}, t) = g(\mathbf{x}, t), & \mathbf{x} \in \partial\Omega, t \in T. \end{cases} \quad (4.4)$$

to demonstrate the correctness, efficiency, and precision of the implementation. The exact solution is given by

$$u(x, y, t; a) = \frac{1}{1 + \exp((x + y - t)/2a)}, \quad \text{on } \Omega \times T, a > 0.$$

where $a > 0$ is the viscosity coefficient. This solution features a sharp transition layer along the line $x + y = t$, propagating diagonally across the domain.

Benchmark. We apply the forward Euler time scheme with $a = 0.005$ and time step $\Delta t = 0.001$. The initial moving meshes include uniform triangular grids of sizes 30×30 , 45×45 , and 60×60 , as well as a 45×45 quadrilateral mesh. For comparison, a fixed uniform triangular grid of size 160×160 is used. See Tab. 7 for L^2 errors and times, Fig. 6 and 7 for the solution and moving mesh respectively.

Type and Density	$t=0.5$	$t=0.75$	$t=1.0$	$t=1.25$	$t=1.5$	Wall Time (s)
Fix Tri 160×160	0.0032488	0.0040798	0.0047631	0.0041900	0.0033862	709.588
Tri 30×30	0.0049148	0.0051815	0.0043073	0.0046847	0.0042645	114.414
Tri 45×45	0.0027004	0.0030660	0.0030052	0.0029330	0.0025511	276.438
Tri 60×60	0.0022169	0.0026554	0.0028656	0.0025694	0.0020576	409.575
Quad 45×45	0.0023646	0.0024993	0.0022470	0.0019312	0.0016308	406.787

Table 7: Convergence results (L^2 errors) for the Burgers' equation with moving mesh.

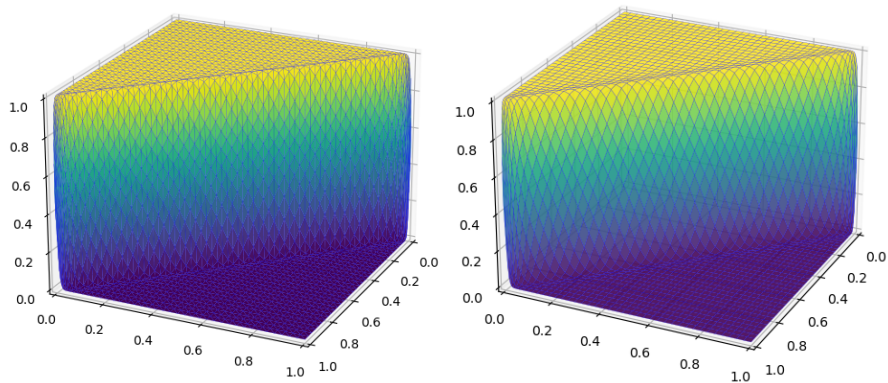


Figure 6: Compares the numerical solution at $t=1.0$ for the 45×45 triangular and quadrilateral moving mesh.

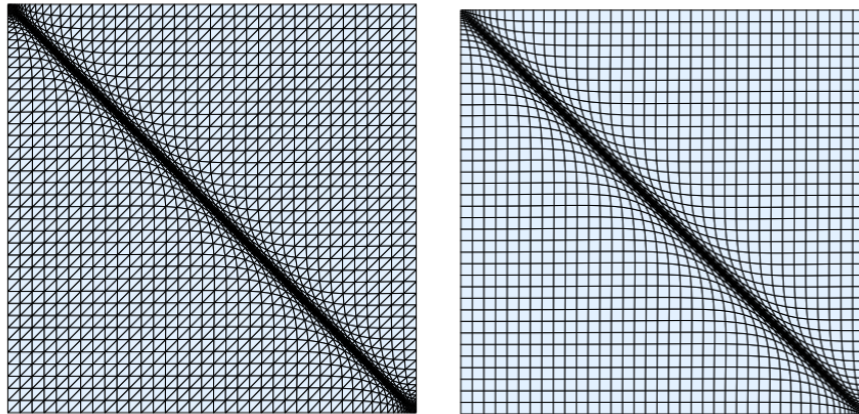


Figure 7: Mesh distribution at $t=1.0$ for the 45×45 triangular and quadrilateral moving mesh. Nodes are clearly concentrates within the sharp transition layer.

Multiple backends. In the second test, we compare computational performance between CPU and GPU execution. With $a = 0.005$ and $\Delta t = 0.001$ over the time interval $[0, 0.25]$, we measure the total runtime on triangular meshes of sizes 60×60 , 80×80 , 120×120 , and 160×160 . The results, summarized in Tab. 8, show that the PyTorch-GPU backend achieves the best performance.

Device	Backend	60×60	80×80	120×120	160×160
CPU	NumPy	36.071	107.114	180.658	387.741
CPU	PyTorch	75.276	121.256	237.256	526.509
GPU	PyTorch	36.602	48.130	76.784	102.323

Table 8: Total runtime (seconds) for the Burgers' equation with different size of moving meshes based on NumPy(CPU) and PyTorch(CPU/GPU).

4.4 Inverse Problem with Learning Automated FEM

Electrical Impedance Tomography (EIT) serves as a typical example of PDE-based inverse problems. It aims to reconstruct the internal conductivity distribution σ of a domain Ω from boundary voltage and current measurements. The governing physical model is described by the elliptic equation:

$$\nabla \cdot (\sigma \nabla u) = 0 \quad \text{in } \Omega,$$

with appropriate boundary conditions. Recovering σ from limited boundary data is notoriously ill-posed, requiring innovative approaches that combine mathematical regularization with data-driven learning.

The γ -deepDSM approach. Inspired by DDSM [14], a novel operator learning framework termed γ -deepDSM [37] was proposed integrating a learnable preconditioning operator with a neural network for enhanced reconstruction. The method consists of two synergistic components (as shown in Fig. 8):

1. Preprocessing via Learnable Fractional Laplace-Beltrami Operator [24]. Boundary data $\tilde{\zeta}_l = g_{D,l} - \Lambda_{\sigma_0} g_{N,l}$ is transformed using an fLB operator with learnable fractional orders γ_l :

$$\mathfrak{L}_{\partial\Omega}^{\gamma_l} \tilde{\zeta}_l = \sum_{k=1}^{K_0} \lambda_k^{\gamma_l} \alpha_k \psi_k,$$

where λ_k, ψ_k are eigenvalues and eigenfunctions of the Laplace-Beltrami operator. This step acts as a preconditioner to amplify high-frequency features critical for reconstruction.

2. Feature Mapping via Neural Network. The preprocessed data $\{\phi_l\}_{l=1}^L$, obtained by solving:

$$-\Delta \phi_l = 0 \quad \text{in } \Omega, \quad \nabla \phi_l \cdot \mathbf{n} = \mathfrak{L}_{\partial\Omega}^{\gamma_l} \tilde{\zeta}_l \quad \text{on } \partial\Omega,$$

are handled as a tensor and fed into a U-Net [31] to reconstruct the conductivity image σ .

Thanks to the PyTorch support of FEALPy, we can easily implement the γ -deepDSM framework by directly embedding FEM code into NN modules, as shown in Lst. 10.

```

1 class DataFeature(nn.Module):
2     ...
3     def forward(self, input: Tensor) -> Tensor:
4         BATCH, CHANNEL, NNBD = input.shape
5         gnv = gnv.reshape(-1, NNBD) # [B*CH, NN_bd]
6         val = self.solver.solve_from_current(gnv)
7         img = self.solver.value_on_nodes(val) # [B*CH, NN]
8         return img.reshape(BATCH, CHANNEL, -1) # [B, CH, NN]

```

Listing 10: A PyTorch NN module containing a FEM solver. The 'self.solver' here is a wrapper for FEALPy code.

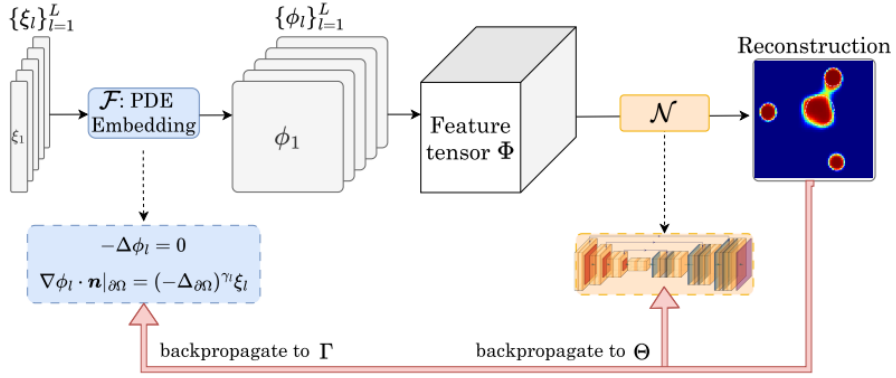


Figure 8: The γ -deepDSM framework.

Results with FEALPy. Experimental results demonstrate that γ -deepDSM achieves approximately 15% improvement in reconstruction accuracy compared to non-learnable approaches across various noise levels and inclusion configurations. The learned fractional orders γ_l adapt to different frequency components in the input data, with higher frequencies corresponding to smaller γ_l values.

This example highlights FEALPy's unified tensor-based architecture, which seamlessly integrates traditional FEM with DL workflows. The work creates a powerful framework for solving challenging inverse problems while maintaining mathematical rigor and computational efficiency.

4.5 Path Planning with Metaheuristic Optimization

In addition to numerical calculations centered on solving direct or inverse PDE problems, FEALPy also integrates a considerable number of intelligent optimization algorithms in the OPT module. Take path planning tasks as an example: results of two

problems, a 2D grid-based and a 3D terrain-based, are illustrated in this subsection to demonstrate the adaptability of FEALPy for implementing intelligent optimization algorithms based on tensor computing frameworks.

PSO on a 2D grid map. A grid-based AGV (Automated Guided Vehicle) path planning problem is considered on a 20×20 map, where cells with value 1 represent obstacles and 0 represent free space. Given the start point (0,0) and end point (19,19), we solve the problem using the Particle Swarm Optimization (PSO) [15] algorithm implemented in FEALPy (Lst. 11). The resulting path is shown in Fig. 9.

```

1 from fealpy.backend import bm
2 from fealpy.pathplanning.model import (
3     PathPlanningModelManager,
4 )
5 from fealpy.opt import ParticleSwarmOpt
6
7 MAP = bm.array([
8     [0, 0, 1, 1, 0, 0, ... , 0],
9     [0, 0, 0, 0, 0, 0, ... , 0],
10    ...
11    [0, 0, 0, 0, 0, 0, ... , 0]
12 ])
13 start_point, end_point = (0, 0), (19, 19)
14
15 # Configure model with PSO
16 options = {
17     'MAP': MAP,
18     'start_point': start_point,
19     'end_point': end_point,
20     'opt_alg': ParticleSwarmOpt
21 }
22 manager = PathPlanningModelManager('route_planning')
23 planner = manager.get_example(2, **options)
24 planner.solver()
25 planner.visualization()

```

Listing 11: 2D path planning model using PSO in FEALPy.OPT. Note that the PathPlanningModelManager generates computational models (such as the planner in this code) as wrappers for the path planning scripts, which improved the readability and usability of the code in basic teaching. Readers can examine its internal implementation to learn how to use the ParticleSwarmOpt algorithm directly.

SAO on a terrain map. A 3D terrain environment is constructed from the dataset ChristmasTerrain.tif, with several cylindrical threat regions to be avoided. Given the start point (800,100,150) and end point (100,800,150), the path was optimized using the Snow Ablation Optimization (SAO) [13] algorithm implemented in FEALPy. Code for this problem is similar, but with a different map type (the threat regions and terrain data), as shown in Lst. 12. The optimized trajectory is shown in Figure 10, which shows the 3D terrain surface and feasible paths.

```

1 ...
2 from fealpy.pathplanning import TerrainLoader

```

```

3 from fealpy.opt import SnowAblationOpt
4
5 terrain_data = TerrainLoader.load_terrain(
6     'ChristmasTerrain.tif'
7 )
8 # [x, y, radius, height]
9 threats = bm.array([
10     [400, 500, 200, 50], ..., [650, 450, 185, 50]
11 ])
12 start_pos = bm.array([800, 100, 150])
13 end_pos = bm.array([100, 800, 150])
14 options = {
15     'threats': threats,
16     'terrain_data': terrain_data,
17     'start_pos': start_pos,
18     'end_pos': end_pos,
19     'opt_method': SnowAblationOpt
20 }
21 ...
22 model = manager.get_example(1, **options)
23 solution, fitness = model.solver(n=10)
24 ...

```

Listing 12: 3D terrain-based path planning using SAO in FEALPy.OPT. The parts that are the same as in the previous example have been omitted.

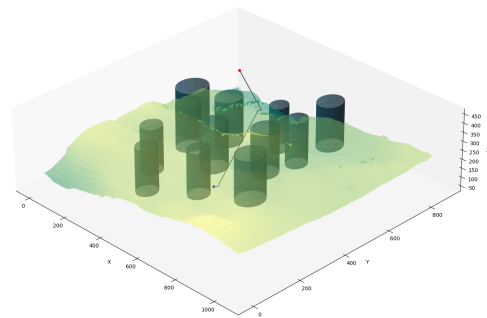
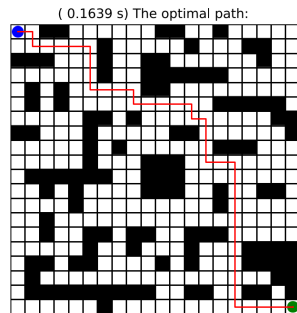


Figure 9: Path planning on a 2D 20×20 grid map, where black squares denote obstacles and the red

Figure 10: The optimized trajectory on a 3D terrain map, obtained by SAO. PSO.

5 Applications

5.1 SOPTX: High-Performance Multi-Backend Topology Optimization

The SOPTX [17] framework was developed based on FEALPy primarily targeting applications in structural topology optimization. SOPTX fully inherits and extends FEALPy's multi-backends feature, diverse numerical algorithm components, and

general-purpose handling capabilities for mesh and geometry. Key technologies such as GPU parallel acceleration, sensitivity analysis based on AD, and high-performance matrix assembly techniques are further integrated based on this foundation, which significantly enhances the computational efficiency of topology optimization problems while ensuring flexibility and extensibility.

SOPTX is built upon a core architecture consisting of four main modules: a Material Module, a Analysis Module, a Regularization Module, and an Optimization Module. These modules communicate and share data through well-defined interfaces, forming a loosely coupled, easily extensible, and multi-backend framework for topology optimization. SOPTX has been successfully applied to solve various topology optimization problems, generating results in excellent agreement with published literature for classic benchmarks, such as the cantilever and MBB beams. SOPTX is also demonstrated to be high performance, with a 67% reduction in assembly time via the high-performance matrix assembly technique, and a $8.1\times$ overall speedup via GPU acceleration compared to CPU in some large-scale 3D problems.

The modular architecture of SOPTX is poised for continued expansion:

- Further enhance the boundary definition and geometric precision of optimization results by integrating technologies such as level-set and phase field solvers, along with adaptive mesh refinement.
- Extend from single-physics structural optimization to more complex, interdisciplinary applications, such as thermo-fluid-structure coupling, by combining with FEALPy's capabilities in solving multiphysics problems.

5.2 FractureX: Flexible and Efficient Phase-Field Fracture Simulation

As an application package built upon the FEALPy library, FractureX provides a comprehensive and modular simulation environment for brittle fracture using the phase-field method (PFM). It is designed to bridge the gap between the theoretical sophistication of PFM and its practical implementation, offering both computational robustness and user flexibility for researchers in computational mechanics.

The core strength of FractureX lies in its modular architecture, which cleanly decouples key physical and numerical components. This design allows users to effortlessly combine different strain energy decomposition models (e.g., isotropic, anisotropic, spectral, and hybrid models [27]), energy degradation functions, and crack surface density functions (AT1, AT2 [36]). Such modularity facilitates rapid prototyping of novel constitutive models and direct comparison between different modeling approaches within a unified codebase.

FractureX adopts an automated adaptive mesh refinement (AMR) strategy driven by a recovery-type error estimator [34], which significantly reduce the cost and improve the accuracy through dynamically focusing the mesh resolution on the fracture region. The main solver includes a robust Newton-Raphson scheme for the strongly coupled displacement-phase-field system. Inherited from FEALPy, GPU acceleration is ready

for large-scale 3D simulations, and AD is also available to skip conventional matrix assembly in rapid tests for new models.

In summary, FractureX exemplifies the power of FEALPy as a foundation for developing specialized scientific computing applications. By abstracting the complexities of the FEM and providing a structured framework for PFM, it lowers the barrier to entry for advanced fracture simulation and serves as a versatile tool for both educational and state-of-the-art research purposes.

6 Conclusions

This work introduced FEALPy, a tensor-centric numerical simulation engine that unifies traditional numerical simulation methods with modern tensor computation/DL frameworks. By organizing computations around a consistent tensor abstraction layer, FEALPy achieves interoperability across multiple backends such as NumPy, PyTorch, and JAX, allowing seamless execution on diverse hardware architectures including CPUs and GPUs.

The modular architecture of FEALPy—comprising the tensor, commonality, algorithmic, and field layers—effectively separates mathematical abstraction from computational realization. This design provides both clarity and flexibility for researchers to implement, extend, and combine numerical algorithms without modifying the underlying data structures. The framework further supports AD through nearly all computational stages, establishing a direct interface between classical PDE solvers and differentiable programming paradigms.

Comprehensive numerical experiments have verified the correctness, efficiency, extensibility and applicability, ranging from elasticity analysis and high-order PDEs to moving mesh computation, inverse problems, and metaheuristic optimization. The derived application frameworks—SOPTX for topology optimization and FractureX for phase-field fracture simulation—further illustrate how FEALPy can serve as a foundation for developing multiple-backends, domain-specific software.

Future developments will focus on enhanced support for multi-physics coupling, large-scale parallel computation, and data-driven numerical modeling. With its unified tensor-based architecture and open, extensible design, FEALPy aims to advance the convergence of numerical analysis, scientific computing, and AI, providing a flexible platform for next-generation computational science.

Associated Content

Data Availability Statement

Source code of FEALPy is available at <https://github.com/weihuayi/fealpy>. And the source code of numerical examples are available at <https://github.com/weihuayi/fealpy/tree/master/example>. The user manual for FEALPy: <http://suanhai.com.cn/intro.html>.

Acknowledgments

This work was supported by the National Key R&D Program of China (2024YFA1012600), the National Natural Science Foundation of China (NSFC) (Grant No. 12371410, 12261131501), and the High Performance Computing Platform of Xiangtan University.

References

- [1] Python array api standard: <https://data-apis.org/array-api/latest/>, 2024.
- [2] Martin S. Alnaes, Anders Logg, Kristian B. Ølgaard, Marie E. Rognes, and Garth N. Wells. Unified form language: A domain-specific language for weak formulations of partial differential equations. *ACM Transactions on Mathematical Software*, 40, 2014.
- [3] R. Anderson, J. Andrej, A. Barker, J. Bramwell, J.-S. Camier, J. Cervený, V. Dobrev, Y. Doudouit, A. Fisher, Tz. Kolev, W. Pazner, M. Stowell, V. Tomov, I. Akkerman, J. Dahm, D. Medina, and S. Zampini. Mfem: A modular finite element methods library. *Computers & Mathematics with Applications*, 81:42–74, 2021.
- [4] Daniel Arndt, Wolfgang Bangerth, Denis Davydov, Timo Heister, Luca Heltai, Martin Kronbichler, Matthias Maier, Jean-Paul Pelteret, Bruno Turcksin, and David Wells. The deal.ii finite element library: design, features, and insights. *Computers & Mathematics with Applications*, 81(3):407–422, 2021.
- [5] Igor A. Baratta, Joseph P. Dean, Jørgen S. Dokken, Michal Habera, Jack S. Hale, Chris N. Richardson, Marie E. Rognes, Matthew W. Scroggs, Nathan Sime, and Garth N. Wells. DOLFINx: the next generation FEniCS problem solving environment. preprint, 2023.
- [6] James Bradbury, Roy Frostig, Peter Hawkins, Matthew James Johnson, Chris Leary, Dougal Maclaurin, George Necula, Adam Paszke, Jake VanderPlas, Skye Wanderman-Milne, and Qiao Zhang. JAX: composable transformations of Python+NumPy programs, 2018.
- [7] Franco Brezzi, Jim Douglas, and L. D. Marini. Two families of mixed finite elements for second order elliptic problems. *Numerische Mathematik*, 47(2):217–235, June 1985.
- [8] Z. Cai, R. Li, et al. Afepack: A general-purpose c++ library for numerical solutions of partial differential equations. *Communications in Computational Physics*, 36(1):274–318, 2024.
- [9] Chunyu Chen, Long Chen, Tingyi Gao, Xuehai Huang, and Huayi Wei. Implementation and basis construction for smooth finite element spaces. *ArXiv*, abs/2507.19732, 2025.
- [10] Chunyu Chen, Long Chen, Xuehai Huang, and Huayi Wei. Geometric decomposition and efficient implementation of high order face and edge elements. *Communications in Computational Physics*, 35(4), 2024.
- [11] Long Chen. *ifem: an integrated finite element methods package in matlab*. Technical report, University of California, Irvine, 2009.
- [12] Long Chen and Xuehai Huang. Geometric decompositions of the simplicial lattice and smooth finite elements in arbitrary dimension. 11 2021.
- [13] Lingyun Deng and Sanyang Liu. Snow ablation optimizer: A novel metaheuristic technique for numerical optimization and engineering design. *Expert Systems with Applications*, 225:120069, 2023.
- [14] Ruchi Guo and Jiahua Jiang. Construct deep neural networks based on direct sampling methods for solving electrical impedance tomography. *SIAM Journal on Scientific Computing*, 43(3):B678–B711, 2021.
- [15] Baole Han, Baosheng Li, and Chuandong Qin. A novel hybrid particle swarm optimization with marine predators. *Swarm and Evolutionary Computation*, 83:101375, 2023.

- [16] Charles R. Harris, K. Jarrod Millman, Stéfan J. van der Walt, Ralf Gommers, Pauli Virtanen, David Cournapeau, Eric Wieser, Julian Taylor, Sebastian Berg, Nathaniel J. Smith, Robert Kern, Matti Picus, Stephan Hoyer, Marten H. van Kerkwijk, Matthew Brett, Allan Haldane, Jaime Fernández del Río, Mark Wiebe, Pearu Peterson, Pierre Gérard-Marchant, Kevin Sheppard, Tyler Reddy, Warren Weckesser, Hameer Abbasi, Christoph Gohlke, and Travis E. Oliphant. Array programming with NumPy. *Nature*, 585(7825):357–362, September 2020.
- [17] Liang He, Huayi Wei, and Tian Tian. Soptx: A high-performance multi-backend framework for topology optimization, 2025.
- [18] Jun Hu, Ting Lin, and Qingyu Wu. A construction of c^r conforming finite element spaces in any dimension. *Foundations of Computational Mathematics*, 24, 10 2023.
- [19] Jun Hu and ShangYou Zhang. A family of symmetric mixed finite elements for linear elasticity on tetrahedral grids. *Science China Mathematics*, 58(2):297–307, February 2015.
- [20] Weizhang Huang. Practical aspects of formulation and solution of moving mesh partial differential equations. *Journal of Computational Physics*, 171(2):753–775, 2001.
- [21] H. Jasak, A. Jemcov, and Z. Tukovic. Openfoam: Open source cfd in research and industry. *International Journal of Naval Architecture and Ocean Engineering*, 1(2):89–94, 2009.
- [22] Robert C. Kirby. Fast simplicial finite element algorithms using Bernstein polynomials. *Numerische Mathematik*, 117(4):631–652, April 2011.
- [23] Jean Kossaifi, Yannis Panagakis, Anima Anandkumar, and Maja Pantic. Tensorly: Tensor learning in python. *Journal of Machine Learning Research*, 20(26):1–6, 2019.
- [24] Mateusz Kwaśnicki. Ten equivalent definitions of the fractional laplace operator. *Fractional Calculus and Applied Analysis*, 20(1):7–51, 2017.
- [25] Ruo Li, Tao Tang, and Pingwen Zhang. Moving mesh methods in multiple dimensions based on harmonic maps. *Journal of Computational Physics*, 170(2):562–588, 2001.
- [26] Ruo Li, Tao Tang, and Pingwen Zhang. A moving mesh finite element algorithm for singular problems in two and three space dimensions. *Journal of Computational Physics*, 177(2):365–393, 2002.
- [27] C. Miehe, M. Hofacker, and F. Welschinger. Phase field modeling of fracture in elastic-plastic solids: Application to ductile fracture. *Computer Methods in Applied Mechanics and Engineering*, 199:2765–2778, 2010.
- [28] J. C. Nédélec. A new family of mixed finite elements in r^3 . *Numerische Mathematik*, 50(1):57–81, January 1986.
- [29] Adam Paszke, Sam Gross, Francisco Massa, Adam Lerer, James Bradbury, Gregory Chanan, Trevor Killeen, Zeming Lin, Natalia Gimelshein, Luca Antiga, Alban Desmaison, Andreas Köpf, Edward Yang, Zachary DeVito, Martin Raison, Alykhan Tejani, Sasank Chilamkurthy, Benoit Steiner, Lu Fang, Junjie Bai, and Soumith Chintala. Pytorch: An imperative style, high-performance deep learning library. *ArXiv*, abs/1912.01703, 2019.
- [30] P. A. Raviart and J. M. Thomas. A mixed finite element method for 2-nd order elliptic problems. In Ilio Galligani and Enrico Magenes, editors, *Mathematical Aspects of Finite Element Methods*, pages 292–315, Berlin, Heidelberg, 1977. Springer Berlin Heidelberg.
- [31] Olaf Ronneberger, Philipp Fischer, and Thomas Brox. U-net: Convolutional networks for biomedical image segmentation[j]. In Nassir Navab, Joachim Hornegger, William M. Wells, and Alejandro F. Frangi, editors, *Medical Image Computing and Computer-Assisted Intervention – MICCAI 2015*, pages 234–241, Cham, 2015. Springer International Publishing.
- [32] Matthew W. Scroggs, Igor A. Baratta, Chris N. Richardson, and Garth N. Wells. Basix: a runtime finite element basis evaluation library. *Journal of Open Source Software*, 7(73):3982, 2022.
- [33] Matthew W. Scroggs, Jørgen S. Dokken, Chris N. Richardson, and Garth N. Wells. Con-

- struction of arbitrary order finite element degree-of-freedom maps on polygonal and polyhedral cell meshes. *ACM Transactions on Mathematical Software*, 48(2):18:1–18:23, 2022.
- [34] Tian Tian, Chunyu Chen, Liang He, and Huayi Wei. Adaptive finite element method for phase field fracture models based on recovery error estimates. *Journal of Computational and Applied Mathematics*, 472:116732, 2026.
- [35] D.M. Williams, L. Shunn, and A. Jameson. Symmetric quadrature rules for simplexes based on sphere close packed lattice arrangements. *Journal of Computational and Applied Mathematics*, 266:18–38, 2014.
- [36] Jian-Ying Wu and Vinh Phu Nguyen. A length scale insensitive phase-field damage model for brittle fracture. *Journal of the Mechanics and Physics of Solids*, 119:20–42, 2018.
- [37] Yangyang Zheng, Huayi Wei, Shuhao Cao, and Ruchi Guo. γ -deepdsm for interface reconstruction: operator learning and a learning-automated fem package, 2024.